

The Two Dimensional Numerical Modeling Of Acoustic Wave Propagation in Shallow Water

Ahmad Zakaria¹, John Penrose¹, Frank Thomas¹ and Xiuming Wang²

¹Centre for Marine Science and Technology, Curtin University of Technology. ²CSIRO Petroleum.

Abstract

This paper describes progress on a two dimensional numerical simulation of acoustic wave propagation that has been developed to visualize the propagation of acoustic wave fronts and to provide time-domain signal representation in shallow water. It is intended that an extension of the work presented here, to account for three-dimensional effects, will later be compared with field results.

The numerical simulation of shallow water acoustic propagation has given rise to a wide variety of modeling techniques with various degrees of accuracy. One technique, involving finite difference methods, is more commonly used in the description of seismic propagation but also occurs in the shallow water propagation literature. This work reported here involves the application of finite difference techniques to model propagation in the time domain, together with associated code to allow wave front visualization.

Introduction

Many researchers have developed numerical interpretations of the wave equations suited to acoustic and seismic propagation (Alford, Kelly, and Boore, 1974; Kelly, Ward, Sven Treitel, and Alford, 1976; Cerjan, Kosloff, and Reshef, 1985; Williams, Rechten, Anderson, 1996; Wu, Lines, and Lu, 1996, Keiswetter, Black, and Schmeissner, 1996; Aleksev, Mikhailenko, 1999). The numerical modeling of seismic data has been used to support interpretations of field data, to provide synthetic data for testing processing techniques and acquisition parameters, and to enhance seismologists' understanding of wave propagation (Keiswetter, Black, and Schmeissner, 1996). For these applications finite-difference methods have often been used.

This report terms the wave equations suited to waves in fluids, acoustic waves and wave in solids such that both shear and compressional, deformations are accounted for are termed elastic waves. Most seismic modeling necessarily uses the elastic wave equations. (Kelly, Ward, Sven Treitel, and Alford, 1976) but the acoustic wave equations have also been used for geophysical modeling techniques (Alford, Kelly, and Boore, 1974). The elastic wave equations are needed to fully account for wave propagation in the seabed but an acoustic wave approximation is often used for seabed sediments when shear velocities are low.

This paper reports on progress in developing a computer program, which deals with the two-dimensional numerical modeling of acoustic wave propagation in shallow water.

Key features of the model at present are:

- (i) The use of acoustic wave equation
- (ii) Time domain modelling
- (iii) A comparison of the use of 2nd and 4th order accuracy

Theory

Acoustic wave equation

A two-dimensional acoustic wave equation can be found using Euler's equation and the equation of continuity (Brekhovskikh, 1960).

$$\frac{\partial p}{\partial t} + \mathbf{r} \cdot c^2 \nabla \cdot \mathbf{u} = 0 \quad \text{Continuity} \quad (1)$$

$$\frac{\partial \mathbf{u}}{\partial t} + \frac{1}{\mathbf{r}} \nabla p = 0 \quad \text{Euler} \quad (2)$$

Where u is the particle velocity, p is the acoustic pressure, $\mathbf{r} = \mathbf{r}(x, z)$ is the density, and $c = c(x, z)$ is the velocity of the acoustic wave in the acoustic media. Substitution of the divergence of the Euler equation and the time derivative of the equation of continuity yield,

$$\frac{\partial^2 p}{\partial t^2} + \mathbf{r} c^2 \left\{ -\bar{\nabla} \left[\frac{1}{\mathbf{r}} \bar{\nabla} p \right] \right\} = \mathbf{d}(r) f(t) \quad (3)$$

$$\frac{\partial^2 p}{\partial t^2} - \mathbf{r} c^2 \left\{ \frac{\partial}{\partial x} \left(\frac{1}{\mathbf{r}} \frac{\partial p}{\partial x} \right) + \frac{\partial}{\partial z} \left(\frac{1}{\mathbf{r}} \frac{\partial p}{\partial z} \right) \right\} = \mathbf{d}(r) f(t) \quad (4)$$

Where $\mathbf{d}(r)$ is the Dirac delta function associated with the position of the source in space and $f(t)$ is the source function.

For homogenous media, the acoustic wave equations can be simplified as follows,

$$\frac{\partial^2 p}{\partial t^2} - c^2 \left\{ \frac{\partial^2 p}{\partial x^2} + \frac{\partial^2 p}{\partial z^2} \right\} = \mathbf{d}(r) f(t) \quad (5)$$

Finite-difference solution

Acoustic wave equation

Finite-difference methods can be applied to the scalar acoustic wave equation. The second time derivative and first spatial derivative of the wave equation can be approximated using a second order central difference approximation as follows,

$$\frac{\partial^2 p}{\partial t^2} = \frac{p_{i,j}^{k+1} - 2p_{i,j}^k + p_{i,j}^{k-1}}{(\Delta t)^2} \quad (6)$$

$$\left\{ \frac{\partial}{\partial x} \frac{1}{\mathbf{r}} \left(\frac{\partial p}{\partial x} \right) \right\}_{i,j}^k = \frac{1}{\mathbf{r}_{i+\frac{1}{2},j}^k} \frac{1}{\Delta x} \left(\frac{p_{i+1,j}^k - p_{i,j}^k}{\Delta x} \right) - \frac{1}{\mathbf{r}_{i-\frac{1}{2},j}^k} \frac{1}{\Delta x} \left(\frac{p_{i,j}^k - p_{i-1,j}^k}{\Delta x} \right) \quad (7)$$

$$\left\{ \frac{\partial}{\partial z} \frac{1}{\mathbf{r}} \left(\frac{\partial p}{\partial z} \right) \right\}_{i,j}^k = \frac{1}{\mathbf{r}_{i,j+\frac{1}{2}}^k} \frac{1}{\Delta z} \left(\frac{p_{i,j+1}^k - p_{i,j}^k}{\Delta z} \right) - \frac{1}{\mathbf{r}_{i,j-\frac{1}{2}}^k} \frac{1}{\Delta z} \left(\frac{p_{i,j}^k - p_{i,j-1}^k}{\Delta z} \right) \quad (8)$$

Where,

$$\frac{1}{\mathbf{r}_{i\pm\frac{1}{2},j}^k} = \frac{1}{2} \left(\frac{1}{\mathbf{r}_{i\pm 1,j}^k} + \frac{1}{\mathbf{r}_{i,j}^k} \right)$$

$$\frac{1}{\mathbf{r}_{i,j\pm\frac{1}{2}}^k} = \frac{1}{2} \left(\frac{1}{\mathbf{r}_{i,j\pm 1}^k} + \frac{1}{\mathbf{r}_{i,j}^k} \right)$$

An acoustic wave equation for homogenous media can be approximated in rectangular coordinates system by the second-order and fourth-order central difference (Alford, Kelly, Boore, 1974; Wang, Personal Communication, 2000) as follows,

$$p_{i,j}^{k+1} = 2(1 - 2\mathbf{g}^2) p_{i,j}^k - p_{i,j}^{k-1} + \mathbf{g}^2 (p_{i+1,j}^k + p_{i-1,j}^k + p_{i,j+1}^k + p_{i,j-1}^k) \quad (9)$$

Where $\Delta x = \Delta z = h$ is the grid size in the x and z directions, respectively and Δt is the time step.

Another alternate expression for higher accuracy uses the fourth-order central difference scheme of the acoustic wave equation. It is more accurate than second-order central difference scheme.

$$p_{i,j}^{k+1} = (2 - 5\mathbf{g}^2) p_{i,j}^k - p_{i,j}^{k-1} + \frac{4}{3} \mathbf{g}^2 (p_{i+1,j}^k + p_{i-1,j}^k + p_{i,j+1}^k + p_{i,j-1}^k) - \frac{1}{12} \mathbf{g}^2 (p_{i+2,j}^k + p_{i-2,j}^k + p_{i,j+2}^k + p_{i,j-2}^k) \quad (10)$$

Where: $\mathbf{g} = \left(\frac{c \Delta t}{\Delta h} \right)$,

A finite-difference scheme will be stable if $\mathbf{g} = 1/\sqrt{2}$ for equation (9) and $\mathbf{g} = \sqrt{3/8}$ for equation (10) (Alford et. al., 1974)

Boundary conditions

Where transparent boundary conditions are involved, we use the method due to Reynolds (1978).

Transparent boundary condition

Left side boundary

$$p_{1,j}^{k+1} = p_{1,j}^k + p_{2,j}^k - p_{2,j}^{k-1} + c_{i,j} \frac{\Delta t}{\Delta x} (p_{2,j}^k - p_{1,j}^k - (p_{3,j}^{k-1} - p_{2,j}^{k-1})) \quad (11)$$

Right side boundary

$$p_{n+1,j}^{k+1} = p_{n+1,j}^k + p_{n,j}^k - p_{n,j}^{k-1} + c_{i,j} \frac{\Delta t}{\Delta x} (p_{n,j}^k - p_{n+1,j}^k - (p_{n-1,j}^{k-1} - p_{n,j}^{k-1})) \quad (12)$$

Surface side boundary

$$p_{i,1}^{k+1} = p_{i,1}^k + p_{i,2}^k - p_{i,2}^{k-1} + c_{i,j} \frac{\Delta t}{\Delta z} (p_{i,2}^k - p_{i,1}^k - (p_{i,3}^{k-1} - p_{i,2}^{k-1})) \quad (13)$$

Bottom side boundary

$$p_{i,m+1}^{k+1} = p_{i,m+1}^k + p_{i,m}^k - p_{i,m}^{k-1} + c_{i,j} \frac{\Delta t}{\Delta z} (p_{i,m}^k - p_{i,m+1}^k - (p_{i,m-1}^{k-1} - p_{i,m}^{k-1})) \quad (14)$$

Nonreflecting boundary condition

We are at present investigating the approach due to Cerjan et al. (1985) which may be summarised as follows

The pressure amplitudes outside the boundary lines must be multiplied by G factor (Cerjan, et.al.1985).

$$G = EXP\left\{-[0.015(20-i)]^2\right\} \quad (15)$$

Where: $1 \leq i \leq 20$

This gives a value of 1 for $i = 20$ or at the nearest boundaries with boundary lines and a value of about 1/250 for $i = 1$ or at the outer boundaries.

Source function

As the source function $f(t)$, a single cycle sinusoid was used.

Results

We present here some of the results of the numerical modeling comprising a comparison between the finite-difference results from second order (7) and fourth order approximations (10) using the transparent boundary condition. The wave front results are also compared with some original results from related acoustic wave simulation work that has been developed by Wang.

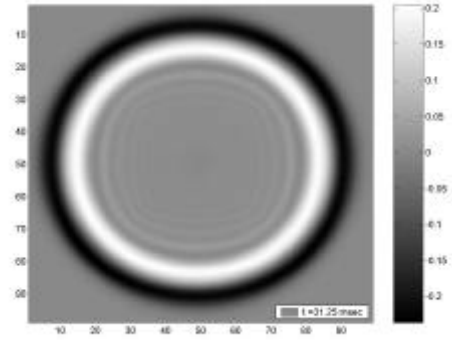


Figure 1.a: (2nd order)

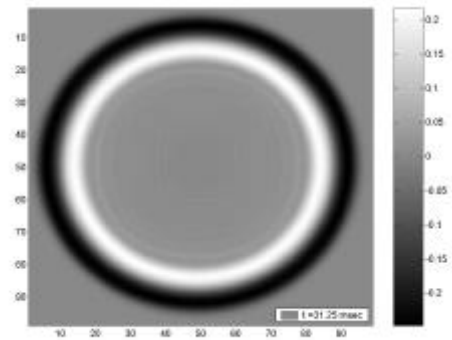


Figure 1.b: (4th order)

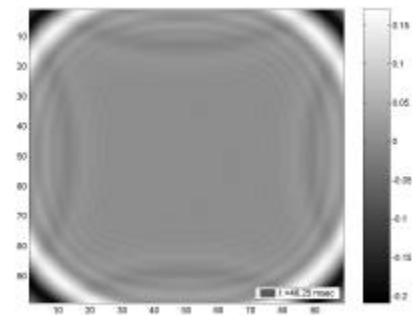


Figure 2.a: (2nd order)

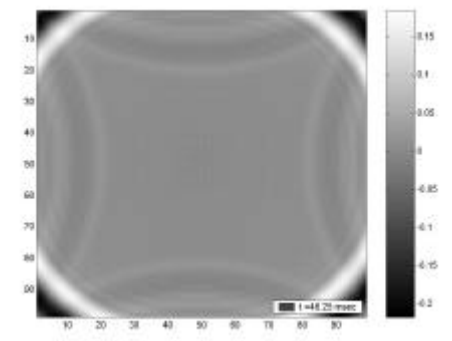


Figure 2.b: (4th order)

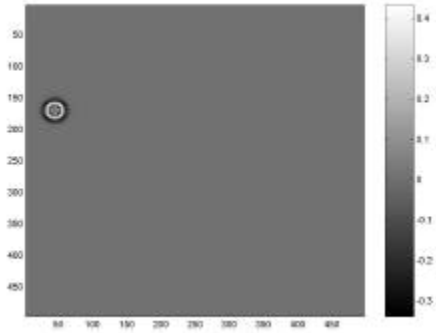


Figure 3: $t = 5$ msec (2nd order)

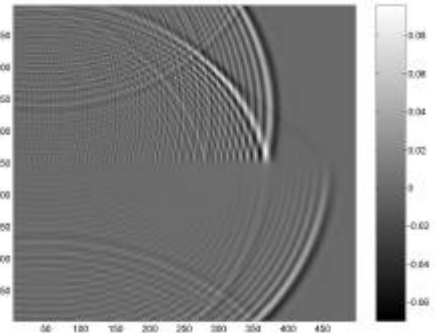


Figure 5.b: $t = 85$ msec (4th order)

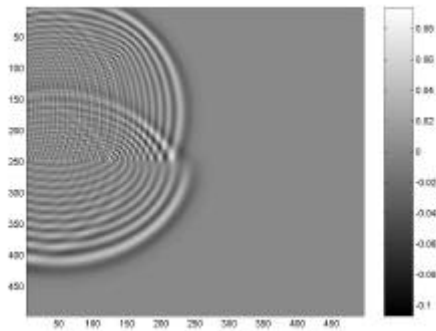


Figure 4.a: $t = 50$ msec (2nd order)

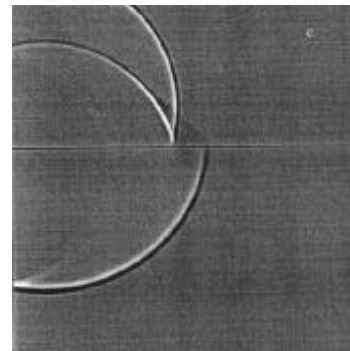


Figure 6.a: $t = 50$ msec (Wang)

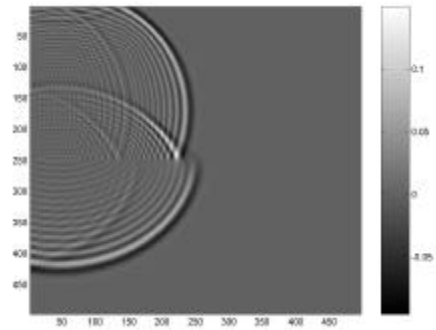


Figure 4.b: $t = 50$ msec (4th order)

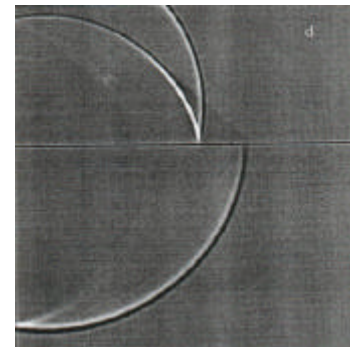


Figure 6.b: $t = 60$ msec (Wang)

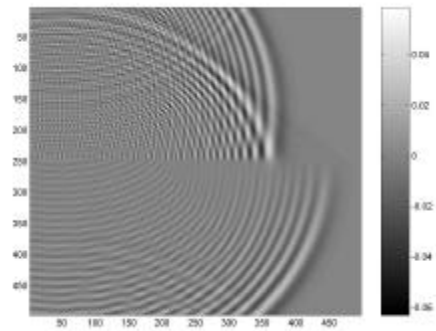


Figure 5.a: $t = 85$ msec (2nd order)

Figure 1.a, 1b, 2a, and 2.b. show wave front simulation results in a homogeneous space represented using 101×101 grid points with $c = 1500$ m/s, $\rho = 1025$ m³/kg, $\Delta x = \Delta z = 1$ m, $\Delta t = 0.025$ msec with a single sinusoid signal of source amplitude $A = 2$ and frequency (f) = 100 Hz. Some reflections are observed. Figure 3 shows the source position used in the simulations represented in figures 4 and 5. Figures 4.a, 4.b, 5.a, and 5.b show the results using 201×201 grid points in a two-layer environment. Velocity c and density ρ in the upper and lower layers are 4000 m/s, 1300 m³/kg and 6000 m/s, 1800 m/s respectively. Here $\Delta x = \Delta z = 2.5$ m, $\Delta t = 0.025$ msec with source amplitude $A = 2$ and frequency (f) = 400 Hz. Figures 6.a and 6.b show acoustic wave front simulation results using 512×512 grid points, due to Wang. The acoustic velocities in upper and

lower layers are 4000m/s and 6000m/s respectively but with constant density throughout. Figures 4.a – 5.b show evidence of dispersion, presently attributed to grid size effects. The effects of incomplete boundary transparency are still apparent. The 4th order results show somewhat less dispersion than those arising from the 2nd order computations. The results also can be compared with Wang’s results in figures 6.a. and 6.b. In all cases direct, reflected refracted and head waves are observed.

Amplitude signals from receivers for the homogeneous media case of figures 1 and 2 are shown as follows,

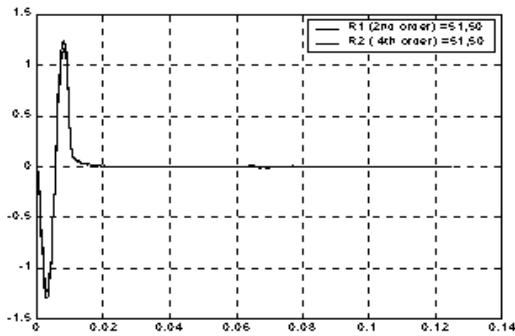


Figure C.1: At position S=51,51;R=5

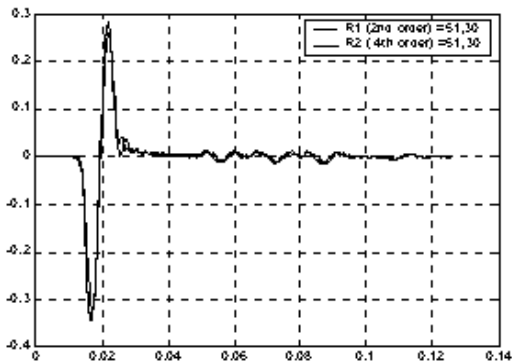


Figure D: At position S=51,51;R=51,30

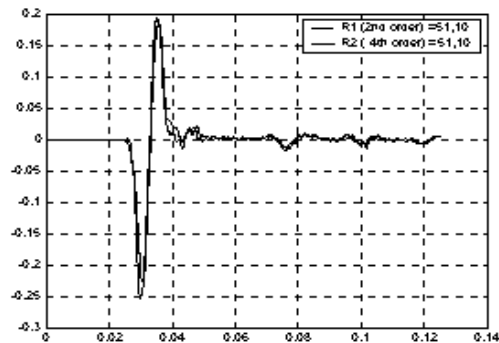


Figure E.1: At position S=51,51; R=51,10

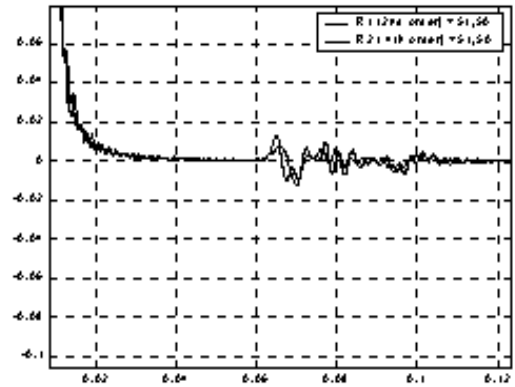


Figure C.2: zoom C.1

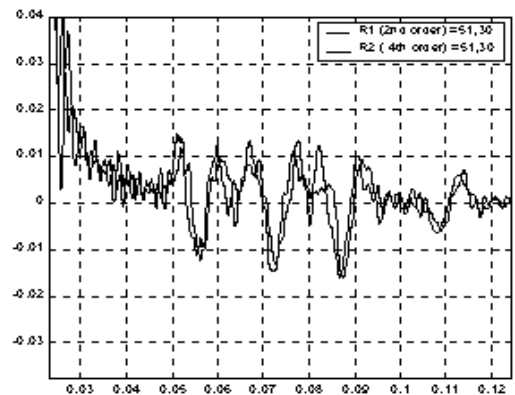


Figure D.2: Zoom D.1

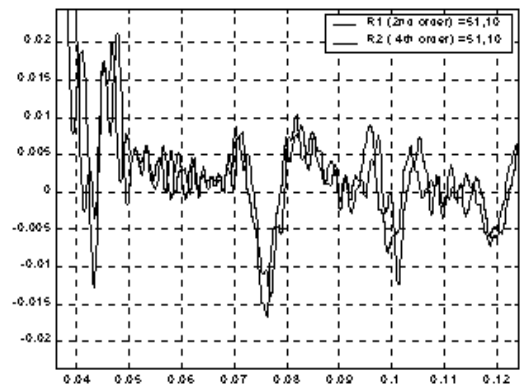


Figure E.2: Zoom E.1

Figures C.1, C.2, D.1, D.2, E.1, E.2 show in the time domain the influences of dispersed waves and transparent boundaries.

The range dependence of acoustic pressure is shown in figure F. This shows the average of the amplitudes of the initial positive and negative pressure excursions P

as a function of range r . The relationship $P(r)$ may be expressed by equation (16),

$$P = a.r^b \quad (16)$$

Curve fitting yields a , b and associated correlation coefficient as shown in the table 1,

Order	a	b	R^2
2 nd	1.2527	-0.4832	0.9982
4 th	2.6650	-0.4471	0.9993
Average	1,9589 \approx 2	-0.4651 \approx -0.5	0.9993

Table.1: Coefficients a and b

Coefficient b is close to the -0.5 value expected for cylindrical spreading.

Conclusions

We have developed 2-D acoustic finite-difference codes for second order in time and second or fourth order in space to model acoustic wave propagation in heterogenous media.

We have presented a comparison between wave fronts developed using 2nd order and 4th order approximations to the acoustic wave equations, shown dispersed wave problems and partial transparent boundary effects. The acoustic modeling shows the expected direct, reflected and refracted and head waves patterns in a two-layer space.

References

- Alford, R. M., Kelly, K. R., and Boore, D. M., 1974, Accuracy of finite-difference modeling of acoustic wave propagation: *Geophysics*, v. 39, no. 6, p. 834-842.
- Kelly, K. R., Ward, R. W., Sven Treitel, and Alford, R. M., 1976, Synthetic Seismograms: A finite-difference Approach: *Geophysics*, v. 41, no. 1, p.2-27.
- Reynold, A. C., 1978, Boundary conditions for the numerical solution of wave propagation problems: *Geophysics*, v.43, p. 1099-1110.
- Williams, R. S., Rechten, Richard D., and Anderson, Neil L., 1996, The one-dimensional elastic wave equation: A finite-difference formulation for animated computer applications to full waveform propagation: *Computers & Geosciences*, v.22, no. 3, p.253-266.
- Cerjan, C., Kosloff, D., Kosloff, R., and Reshef, M., 1985., A nonreflecting boundary condition for discrete acoustic and elastic wave equations: *Geophysics*, v. 50, no. 4, p. 705-708.
- Brekhovskikh, L. M., 1960, *Waves in layered media*: Academic Press, New York, p.171.